Curve Boxplot: Generalization of Boxplot for Ensembles of Curves

Mahsa Mirzargar, Ross T. Whitaker, *Senior Member, IEEE*, and Robert M. Kirby, *Member, IEEE*
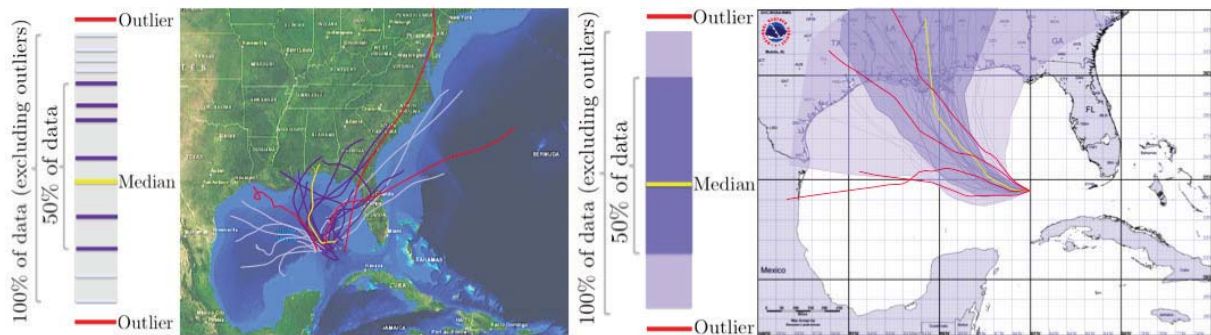

Fig. 1. Visualization of the order statistics of 27 historic hurricane tracks originating in the Gulf of Mexico between 1920 − 2012 (left) and a *curve boxplot* visualization of an ensemble of 50 simulated hurricane tracks (right).

Abstract— In simulation science, computational scientists often study the behavior of their simulations by repeated solutions with variations in parameters and/or boundary values or initial conditions. Through such simulation ensembles, one can try to understand or quantify the variability or uncertainty in a solution as a function of the various inputs or model assumptions. In response to a growing interest in simulation ensembles, the visualization community has developed a suite of methods for allowing users to observe and understand the properties of these ensembles in an efficient and effective manner. An important aspect of visualizing simulations is the analysis of derived features, often represented as points, surfaces, or curves. In this paper, we present a novel, nonparametric method for summarizing ensembles of 2D and 3D curves. We propose an extension of a method from descriptive statistics, data depth, to curves. We also demonstrate a set of rendering and visualization strategies for showing rank statistics of an ensemble of curves, which is a generalization of traditional *whisker plots* or *boxplots* to multidimensional curves. Results are presented for applications in neuroimaging, hurricane forecasting and fluid dynamics.

Index Terms—Uncertainty visualization, boxplots, ensemble visualization, order statistics, data depth, nonparametric statistic, functional data, parametric curves

---

1 INTRODUCTION

In many applications, scientists use mathematical or conceptual models to overcome the complexity of real-world physical phenomena. Recent advances in computational power and the development of high performance computing techniques have made it feasible to run numerical simulations significantly faster. As a result, a simulation ensemble can be done repeatedly for large sets of different parameter values within time frames that are now practical. When the parameter space for a simulation is too large or too complex to be explored completely, scientists often rely on an ensemble of runs to i) explore the potential outcomes of the model or ii) hypothesize about the deficiencies in the model. Ensembles are also used to account for different types of uncertainties caused in different stages of knowledge acquisition, such as deficiencies in the model, unknown parameters and limited numerical accuracy.

With an increase in the complexity and dimensionality of data, visualization has become an integral and essential part of data analysis, and it continues to facilitate knowledge discoveries in various applica-

• *Mahsa Mirzargar is with the Scientific Computing and Imaging Institute, University of Utah, Salt Lake City, UT 84112. E-mail: mirzargar@sci.utah.edu.*
• *Ross T. Whitaker and Robert M. Kirby are with the Scientific Computing and Imaging Institute and School of Computing, University of Utah, Salt Lake City, UT 84112. E-mails: {whitaker, kirby}@cs.utah.edu.*

tions. If designed properly, visualizations can help the user discover or highlight the characteristic features of the data. As the number of applications using ensembles grows, the need for new techniques for visualizing ensembles is also increasing. An ensemble visualization scheme needs to respect the variability between ensemble members and convey such variability properly to the user. In various applications, domain experts are typically interested in specific *derived* features of the data rather than the whole simulation field. Visualization of feature sets requires special treatment as specific criteria need to be satisfied [60]. The particular choice of the feature of interest depends on the application domain and the questions being asked. For instance, isocontours are a typical derived quantity of interest for scalar fields whereas pathlines as parameterized curves are considered as one of the dominant feature sets for flow fields.

Visualizing the uncertainty present in an ensemble requires proper modeling of the variability among the ensemble members. The uncertainty (or the variability) is often modeled using probability theory [50]. An ensemble is considered to be an empirical representation or sampling of the underlying unknown distribution of the data. Extensive studies on the statistical analysis of ensembles can be found in the literature, including both parametric and nonparametric statistical analysis methods. Using parametric methods often results in strict assumptions about the underlying distribution and hence can potentially deteriorate the representation of the intrinsic variability present in the ensemble. Therefore, nonparametric statistical analysis tools are often more suitable to study the variability of an ensemble [45]. Among various nonparametric methods, *descriptive statistics* summarizes the main features of an ensemble with few or no assumptions about the underlying probability distribution—and therefore is robust to the type of distribution and in the presence of outliers [8]. Furthermore, the concept of data depth has been proposed as a natural mathematical

concept by which to derive robust descriptive statistical summaries of an ensemble [62]. Correspondingly, the boxplot visualization adapted to the concept of data depth has been proposed as a simple data exploratory analysis tool for various types of data including multivariate points [48], functional data [54] and isocontours [60].

In this paper, we propose a statistical analysis tool using the concept of data depth for studying ensembles of parameterized curves. We demonstrate how this method can be used to derive robust statistical summaries allowing analysis of an ensemble of parameterized curves including particle trace pathlines. We additionally propose a boxplot-based visualization scheme called a *curve boxplot* as a simple data-exploratory analysis tool to provide both quantitative and qualitative summaries of the variability present in an ensemble of parameterized curves. To demonstrate the utility of our proposed method, we provide a detailed discussion of curve boxplot visualization techniques in comparison with various state-of-the-art visualization techniques in several applications, including tractography imaging, hurricane track prediction and fluid dynamics. Our contribution builds upon previous data depth analysis techniques that aim to provide robust and descriptive statistical representation of ensembles.

2 BACKGROUND AND RELATED WORK

As uncertainty quantification becomes an integrated component in different areas of science, uncertainty visualization has been advocated as one of the top challenges in visualization [26, 40, 31]. Our work is closely related to topics from ensemble visualization, flow field visualization, computational geometry, and visualization of uncertain vector fields and their feature sets. We provide a brief review of the nominal work from each of these topics.

Uncertainty visualization for isosurfaces as one of the dominant feature sets of scalar fields has received significant attention [15, 23]. A class of uncertainty visualization techniques use point-based primitives such as fuzziness [22] or colors [15] to convey the positional uncertainty associated with volumetric data and surfaces. These methods provide qualitative indications about the uncertainty associated with the data, but they fail to provide any quantitative information. Therefore, recent efforts have been devoted to using statistical analysis techniques in order to provide *quantitative* information about the uncertainty present in the data. Parametric models have been used to approximate Level Crossing Probabilities (LCP) [46], based on which the probabilistic marching cubes algorithm was proposed [47] and deployed for ray casting applications [43] and extended for approximation of global correlation [44]. This body of work provides quantitative interpretation of the uncertainty with a parametric model assumption. Reliance on parametric models restricts the capability of capturing the underlying variability in the presence of outliers or general distributions. Recently, a nonparametric kernel density estimation method [45] has been proposed for ensemble-based isosurface visualization. Although the proposed approach provides more flexibility in estimating more general distributions than normal distribution, the efficiency and effectiveness of such methods rely heavily on parameter tuning.

The analysis of flow fields and their derived features plays a vital role in different simulation science applications such as computational fluid dynamics (CFD), medical imaging and numerical weather prediction [14, 49, 19]. Pathline and streamline visualization (as instances of curves) is one of the most important tools for studying the intrinsic properties of a vector field, and hence has received significant attention [59]. One of the main challenges in the visualization of an ensemble of trajectories or streamlines is the issue of *visual clutter*. This issue has been addressed by a number of techniques focusing on a subset of the ensemble of pathlines through preprocessing steps such as streamline bundling [61], view-dependent rendering [36], selective positioning of the seed points [37] or rendering techniques such as density projection method [29]. These techniques are mainly designed to reduce the complexity of the ensemble of pathlines while preserving the salient features of the underlying vector field in the absence of uncertainty. Therefore, these pathline ensemble visualization techniques are not well suited to characterization of the uncertainty associated

with an ensemble of pathlines derived from an uncertain vector field.

Visualization of flow fields and their feature sets in the presence of uncertainty poses new challenges in comparison to conventional flow field visualization. Various visualization techniques have been proposed to study and visualize uncertain vector fields including texture-based techniques [9], comparative flow visualization [32, 57] and ensemble visualization techniques for time varying flow fields [24]. These techniques mainly use analysis and visualization of various feature sets of flow fields in order to study the uncertain vector field. Probabilistic modeling and statistical analysis have been deployed for visualization of various feature sets of vector fields [42]. For instance, extraction and visualization of vortex cores [39], sink and sources [38] extracted from uncertain vector fields have been studied in a probabilistic framework. In our work, we focus on a specific type of feature set from an uncertain vector field, namely an ensemble of pathlines, streamlines, or trajectories, all of which are heavily used in a variety of applications [14, 49, 51] and often times represented as parameterized curves. As mentioned earlier, conventional streamline visualization techniques do not lend themselves to proper characterization of the uncertainty associated with an ensemble of pathlines as parameterized curves. Direct ensemble visualization techniques have been proposed and shown to be effective in characterizing the uncertainty present in an ensemble of pathlines in applications such as weather forecasting [51], hurricane track prediction [14], and tractography [49]. Even though direct visualization of ensembles has been shown to be informative in specific applications, it fails to provide any quantitative measure of aggregation or dispersion between ensemble members and places cognitive burden on the user to interpret the variability present in the ensemble [14]. Similar to level-set crossing probabilities for modeling positional uncertainty of isosurfaces in a scalar field, the spatial distribution of pathlines has been studied and visualized for blood flow measurements [19] and tractography applications [41] as an alternate visualization scheme to direct ensemble visualization. This class of methods provides quantitative summaries of an ensemble of pathlines while the volume rendering of the probability map provides only a qualitative visualization of the potential position of the pathlines.

Another class of closely related, but distinct, analysis techniques in the computational geometry literature aims to study curves purely as geometrical objects. This class of statistical analysis techniques typically relies on curve similarity metrics [11, 5, 17]. These metrics entail registration, deformation [35], alignment [52] and, in some cases, clustering [20], in order to summarize geometric properties of an ensemble. These methods provide an important suite of analysis tools in applications such as medical imaging and statistical shape analysis [28]. However, the analysis of an ensemble of curves through alignment [52] and deformation has two drawbacks: i) the alignment processes themselves are nonlinear optimizations and are often sensitive to parameters, initializations, and application-specific assumptions; and ii) alignment-based methods represent variability only indirectly, through some subsequent analysis of the coordinate transformations or deformations needed to align.

In this work, we propose a more direct approach for statistical analysis of curves. We propose a new methodology (that complements more heavyweight methods) to study and visualize the variability present in an ensemble of curves in a more general setting based on the generalization of the notion of *data depth*. Data-depth analysis and boxplot visualization have been studied and successfully applied to ensembles of various data types. In the next section, we provide a self-contained introduction to the notion of data depth as the building block for our proposed generalization of band depth.

3 DATA DEPTH AND ITS GENERALIZATIONS

Nonparametric statistical analysis methods are a branch of statistics in which there is no (or minimal) model assumption regarding the underlying distribution, which will in turn provide statistical information that is more faithful to the data. Many nonparametric methods have been designed for studying the underlying distribution that gave rise to the ensemble, whereas often the domain experts are interested in *robust* statistical summaries of the ensemble. Descriptive statistics, a

class of nonparametric statistical analysis tools, is designed to provide the *main features* of an ensemble without estimating or representing the underlying distribution.

Data depth is an elegant and powerful method to derive descriptive statistics such as ordering and percentile information with few assumptions about the underlying distribution. Moreover, a proper generalization of the concept of data depth for multivariate and complicated data types such as functions and isocontours has been shown to be sensitive to complex features such as *shapes* [60, 54]. The feature-sensitivity of the notion of data depth guarantees the robustness of the statistical summaries in the presence of outliers and noise [8]. We will formally introduce the notion of data depth and *boxplots* as a simple and effective ensemble visualization technique that represents the statical summaries provided by the data depth. Data depth introduction will provide the fundamental concepts required for the introduction of the generalization of band depth for multivariate curves.

Given an ensemble of data drawn from a distribution F, data depth quantifies how *central* (or deep) is a particular sample within the cloud of the sampled data. The deeper samples are considered more representative of the ensemble and are assigned high depth values whereas samples farther away from the rest of the ensemble are considered to be outliers and are correspondingly assigned lower depth values. Therefore, the notion of data depth provides a *center outward ordering* (also known as order statistics) for an ensemble of sampled data.

The order statistics induced by data depth can be used to provide robust, descriptive statistical information about the ensemble including the most representative ensemble member (*i.e.*, the median), percentile information and also detection of the potential outliers. In the univariate case, merely sorting the values provides enough information to induce the depth values. The univariate boxplot introduced by Tukey [55] is a simple data-exploratory analysis tool designed based on the notion of data depth to summarize the descriptive statistical quantities induced from the ensemble such as median, first and third quartile (i.e., 50% of the data), nonoutlying minimum and maximum values (*i.e.*, 100% of the data), and the potential outliers. A typical boxplot is represented in Figure 2.
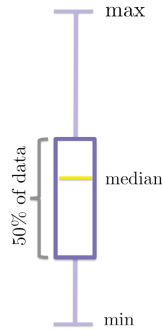
Fig. 2.   Boxplot: a data exploratory visualization tool.

The extension of *sorting* to higher dimensions or more complicated data types such as functional data is a nontrivial task, and therefore proper measures of data depth must be devised based on the type of the data and the application. There are various generalizations for the notion of data depth to higher dimensions [48, 62, 30] from which the notion of *functional band depth* is specifically designed for ensembles of functions [33]. The main distinction between the functional band depth in comparison with other generalizations of the data depth to higher dimensions is that functional band depth goes beyond pointwise analysis of functional data. Functional band depth provides a measure of centrality of a function among an ensemble of functional data that is both sensitive to the *shape* and the *position* of a function in comparison to the rest of ensemble members. Based the notion of functional band depth, functional boxplot has been proposed as an extension of the univariate boxplot [54].

3.1   Functional Band Depth

In its simplest form, a function is defined as a 1D mapping from a subset of the real line called the domain to another subset of the real line called the codomain as:

$$f : \mathscr{D} \mapsto \mathscr{R}, \quad \mathscr{D}, \mathscr{R} \subset \mathbb{R}. \qquad (1)$$

Pointwise statistics of ensembles of functional data will underestimate the correlation between values of the function over its domain and global features such as the shape of the function. Therefore, *centrality* of a function among an ensemble of functions should be evaluated

based on all the values in the domain. Functional band depth is an elegant and mathematically well-defined statistical concept that defines a measure of centrality of a function among an ensemble of functions based on its graphical representation. Considering an ensemble of n functions, $\{f_1(x), f_2(x), \cdots, f_n(x)\}$, the band depth of each ensemble member is defined as the probability of the inclusion of its graphical representation within the *band* formed by a random selection of j other functions from the ensemble. The band in this context is defined as the region on the plane enclosed by j functions as:

$$B\big(f_1(x), \cdots, f_j(x)\big) =$$
$$\{(x,y) : x \in \mathscr{D}, y \in \mathscr{R}, \min_{k=1 \cdots, j} f_k(x) \le y \le \max_{k=1, \cdots, j} f_k(x)\}. \quad (2)$$

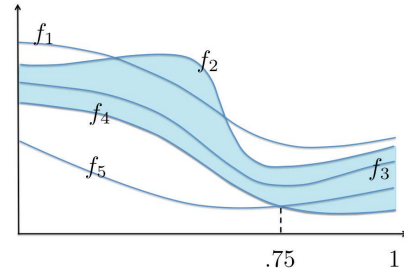The band formed by two functions is shown in blue in Figure 3. An

Fig. 3.   Demonstration of an ensemble of five functions. The band formed by f_2 and f_4 is shaded in blue. Notice that f_3 is fully contained in the band, whereas f_5 falls inside the shaded region (i.e., the band) only 25% of the time.

arbitrary function $g(x)$ lies in the band formed by j randomly selected functions $f_1(x), \cdots, f_j(x)$ only if it satisfies the following property:

$$g(x) \subset B(f_1(x), \cdots, f_j(x)) \quad iff$$
$$\{\forall x \in \mathscr{D} \min_{k=1, \cdots, j} f_k(x) \le g(x) \le \max_{k=1, \cdots, j} f_k(x)\}. \quad (3)$$

For any fixed value of $j \ge 2$, the band depth of a function $g(x)$ among the ensemble of functions can be defined as the probability of the inclusion of its graphical representation in random bands formed by j other ensemble members:

$$BD_j(g(x)) = \text{Prob}[g(x) \subset B(f_{i_1}(x), \cdots, f_{i_j}(x))], \quad 1 \le i_1 \le \cdots, \le i_j \le n \quad (4)$$

where $\text{Prob}[\cdot]$ denotes the probability and the double indices denote a random selection of j functions from the ensemble. The indicator function associated with Eq. (3) can be viewed as a binary random variable. Therefore, the probability $\text{Prob}[\cdot]$ can be computed by the fraction of the bands for which Eq. (4) is satisfied. Intuitively, functions close to the *center* of the distribution have a higher likelihood of being contained in a random band compared to the functions far from the center of the distribution. The value for j and the number of random bands are the two parameters that affect the robustness of the computed data depth values. It has been shown that using different j values to compute the depth values as:

$$BD_J(g(x) = \sum_{j=2}^{J} BD_i(g(x)), \quad (5)$$

can provide more robust depth values [54]. On the other hand, the number of random bands used to compute the depth values should be large enough to prevent degenerate cases. If the number of random bands formed by the ensemble members is low, many of the ensemble members will be assigned with similar (and potentially zero) depth values. One can use all possible bands formed by the ensemble members to compute the band depth values [54]. For instance, for an ensemble of size 10 and $j = 2$ one can form $C(10, 2) = 45$ bands using *any* two ensemble members to compute the band depth for each of the ensemble members.
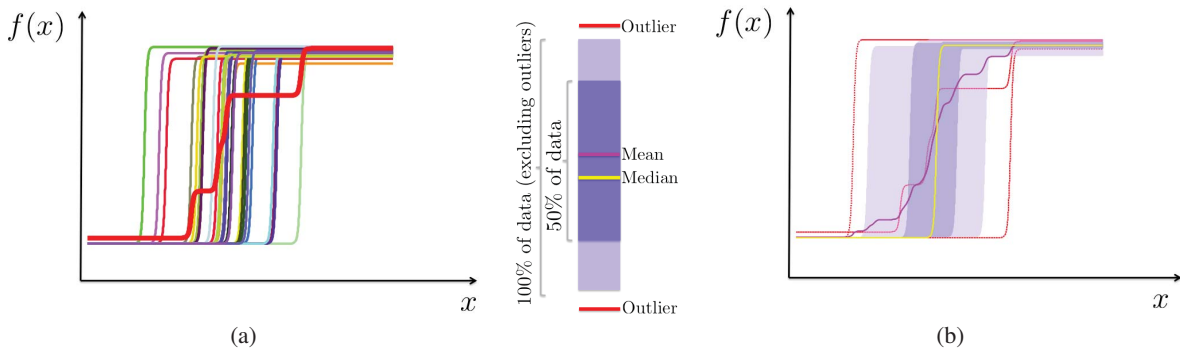
Fig. 4. Illustration of a functional boxplot: (a) An ensemble of 35 canonical step functions where the ensemble members are colored in random. The ensemble is generated by randomly perturbing the horizontal position of the jump. A single outlying example has been generated whose shape is significantly different from the rest of the ensemble. This ensemble member has been highlighted in red (b) A functional boxplot visualization of the ensemble [54]. The coloring scheme follows the 1D boxplot visualized.

As mentioned earlier, one of the main characteristic features of the band depth definition is its *shape* and *position* sensitivity. Ensemble members with significant differences between their positions and the rest of the ensemble members or with too much shape variability are flagged as outliers (red curves in Figure 4). The purple line in Figure 4(b) represents the point-wise mean of the ensemble, which appears to be very different from any of the other ensemble members. This example illustrates that in the presence of outliers, the mean of the ensemble is not a good representative of the ensemble, which is an established concept in the statistical literature [16].

In the presence of noise that will translate into too much variability among the ensemble members or limited number of samples in the ensemble, the data depth values can be very low or close to zero simply because not many ensemble members are fully contained in the bands. In order to overcome this challenge, a more flexible definition of band depth, called the *modified band depth*, was proposed [33]. The modified band depth measures the portion of time that a function lies inside the band. For instance, f_5 in Figure 3 is not fully contained, but it falls inside the colored band 25% of the time. Modified band depth provides more reliable results and prevents degeneracy in the presence of too much variability among the ensemble members in the price of reducing the shape sensitivity of the method. Modified band depth will allow functions that are *approximately* (and not fully) in the band to be assigned with nonzero depth values (*i.e.*, relaxation of the binary evaluation of Eq. (4) into a percentage).

Motivated by the widespread use of derived features of scalar fields in scientific visualization, the notion of band depth has been generalized to sets and isocontours based on which contour boxplot visualization has been proposed [60]. The notion of band depth can also be extended for ensembles of dense fields of data. A field of data can be represented as a *surface*: $S : \mathcal{D} \mapsto \mathcal{R}$ where $\mathcal{D} \subset \mathbb{R}^2$ and $\mathcal{R} \subset \mathbb{R}$. One can use volume-based surface band depth [54] for statistical analysis of ensemble of fields of data (*i.e.*, surfaces) [21]. In the next section, we will define a generalization of the notion of band depth for parameterized curves in higher dimensions.

Statistical properties of the notion of data depth and specifically band depth have been widely studied in the statistics literature [30] where it has been shown that the sample mean of the probability associated with Eq. (4) converges to its expected value as the size of the ensemble goes to infinity. The ensemble member with the maximum depth value will converge to the center of a symmetric distribution (*i.e.*, the median of the distribution), whereas the depth value for an outlier will converge to zero. Thus, the descriptive statistics induced by data depth and boxplot visualizations provide a robust, interpretable representation of a distribution.

4 METHODS

4.1 Generalization of Band Depth for Multivariate Curves

Just as the upper and lower envelope of a set of scalar functions defines a band, multivariate functions define a band by the geometric extent of the points in the codomain. Thus, a natural extension of the notion of
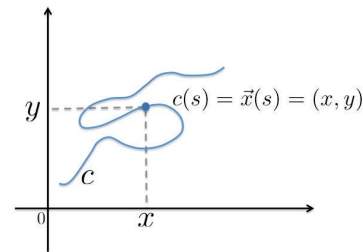

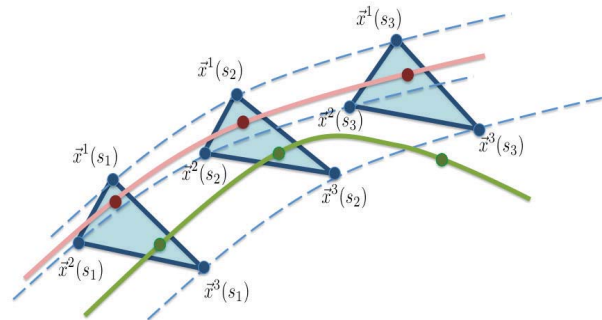Fig. 5. A typical 2D parameterized curve.

Fig. 6. The band formed by three dashed curves. The corresponding points along the curves forming the band have been highlighted in blue. The red curve is fully contained in the band based on the definition given in Eq. (8) whereas the green curve does not fall inside the band.

band depth can be defined for multivariate functions and parameterized curves in higher dimensions (presented here, and also developed independently by Pintado *et al.* [34]), is determined by containment in the simplex or convex hull formed by points in the codomain. However, this assumes a predefined parameterization for every curve. A parameterized curve can be defined in terms of an independent parameter s as:

$$c(s) = \vec{x}(s) \qquad c : \mathcal{D} \mapsto \mathcal{R} \qquad \mathcal{D} \subset \mathbb{R}, \mathcal{R} \subset \mathbb{R}^d \qquad (6)$$

where $\vec{x} \in \mathbb{R}^d$ is the spatial location of the curve at a specific point in the domain (see Figure 5). As the value of the independent parameter s changes in the domain $\mathcal{D}$, c traces a curve in $\mathbb{R}^d$. In what follows, we introduce the generalization of the notion of band depth for parameterized curves.

Considering an ensemble of n curves in $\mathbb{R}^d$: $\{c_1, \cdots, c_n\}$, where the correspondence between the ensemble members is established based on the independent parameter s, we can define the generalized notion of band depth using a new definition for the band and the concept of

inclusion in the band. A band formed by j ensemble members in this context can be defined as:

$$B(c_1(s), \cdots, c_j(s)) = \\ \{(s, \vec{y}) : s \in \mathcal{D}, \vec{y}(s) \in \mathcal{R}, \vec{y}(s) \in \Delta(\vec{x}^1(s), \cdots, \vec{x}^j(s))\}, \quad (7)$$

where $\vec{x}^j(s)$ denotes the point on $c_j(s)$ and $\Delta(\vec{x}^1(s), \cdots, \vec{x}^j(s))$ denotes the geometrical convex hull formed by $\vec{x}^1(s), \cdots, \vec{x}^j(s)$ in $\mathbb{R}^d$ (see Figure 6). Note that in the functional band depth, the band is defined as the region enclosed by the graph of j functions. Equivalently, we have defined the band as the region enclosed between the corresponding points along j curves in $\mathbb{R}^d$ using the notion of a convex hull. Now, we can introduce the notion of *inclusion* in the band in $\mathbb{R}^d$. A parameterized curve $g(s)$ is fully contained in the band if all the points along $g(s)$ satisfy the following relation:

$$g(s) \subset B(c_1(s), \cdots, c_j(s)) \quad iff \\ \{\forall s \in \mathcal{D} \quad \vec{x}(s) \in \Delta(\vec{x}^1(s), \cdots, \vec{x}^j(s))\}. \quad (8)$$

Similar to functional band depth, the measure of centrality of an ensemble member is defined as the sample probability of its inclusion in random bands formed by a random selection of j other ensemble members:

$$BD^j(g(s)) = \text{Prob}\left[g(s) \subset B(c_{i_1}(s), \ldots, c_{i_j}(s))\right] \quad 1 \le i_1 \le \cdots \le i_j \le n. \quad (9)$$

The choice of j for the number of the ensemble members to form the band in $\mathbb{R}^d$ needs to be at least $d+1$ to define proper convex hulls in Eq. (8). If $j = d+1$, the convex hull in Eq. (8) defines a simplex that establishes the connection of this notion of band depth to the simplicial band depth [30]. Consequently, one can use any other notion of centrality defined for multivariate points to replace the convex hull relation in Eq. (8). For instance, one might instead use the definition constructed from half-spaces [55]. It is also important to note that this definition of band depth for parameterized curves coincides with the functional band depth definition when the codomain is defined as a subset of $\mathbb{R}$.

4.2 Boxplots for Multivariate Curves

Here we describe the construction of boxplots for multidimensional-parameterized curves. In applications such as computational fluid dynamics (CFD) or numerical weather prediction (*e.g.*, hurricane track prediction), evolution time is a *natural* choice for parameterization of pathlines as curves, and this will uniquely determine how points are compared in the range (to test for containment, as above). In situations where time does not provide a natural parameter space, one can reparameterize the ensemble of curves based on a given or application-specific criteria as a preprocessing step prior to data-depth analysis. Some of the common choices for reparameterization includes arc length parameterization [58] or optimization of properly designed cost functions [53]. The choices of parameterizations present tradeoffs. The time-based parameterization specifically accounts for the different actual speeds of the curves or pathlines (*e.g.* hurricane speed), whereas the arc-length parameterization ignores the underlying speed along a curve and considers only its shape. These choices are inevitably application dependent; here we will consider the different alternatives in the context of several different applications.

For all applications discussed in the following section, the data depth analysis was carried out using the modified version of the band depth definition. The notion of functional band depth is stable with respect to different values of j [54], we also observed the same behavior for its generalization for curves. For the 2D examples, we have used three points to form the convex hull (*i.e.*, a triangle) and in the 3D case, we have chosen to use $j = 5$. Smaller values for j allow for more shape sensitivity of the approach and are significantly faster to compute [33]. In all our experiments we used *all* the bands formed by subsets of the ensemble members. The depth values induced from data depth analysis can then be used to order (or rank) the ensemble members based on which we propose a generalization of univariate boxplot

visualization that we call *curve boxplot*. In a curve boxplot visualization, the median and outlier ensemble members are rendered using the color convention used for the univariate boxplot demonstrated in Figure 4. Multiple design choices can be used to represent the 50% and 100% band. One can render the ensemble members falling inside the 50% (or 100%) band with a distinct color. Individual coloring of the curves is desirable in situations where some topological phenomena such as bifurcations emerge. On the other hand, in order to provide an equivalent representation of the 50% band to the univariate boxplot and functional boxplot we used CSG (Constructive Solid Geometry) union operator to represent the contiguous 50% *band* swept by the 50% deepest ensemble members. In order to construct a solid region (which is not necessarily convex), we first constructed our primitives as all the convex hulls formed by 2 consecutive and corresponding points along the 50% deepest ensemble members. This will assure that the region swept by these members is fully covered. Then, these convex hulls have been combined to a single solid region (i.e., the 50% band) using sequential union operations.

We detect the outliers as the members whose depth value is smaller than the inflation of the range of depth values for the 50% band by a factor of three [56]. The outliers are shown in red in all examples. In the 2D examples, we also render the 100% band in a distinct color; however, to prevent cluttered images in the 3D examples, we have chosen to show the nonoutlier ensemble members beyond 50% band individually with a lighter shade of blue. This approach will help the user to better track the position of the ensemble members.

5 RESULTS AND APPLICATIONS

In this section, we discuss experimental results to demonstrate the utility of the curve boxplot visualization to study the variability present in an ensemble of parameterized curves and pathlines in various applications. We present observations on the method from users who studied these visualizations relative to the state of the art. Comparisons will be provided between alternative application-specific approaches used to visualize ensembles and we will comment on why boxplot visualization can be a proper alternative ensemble visualization scheme. For each of the applications, the advantages of the data depth analysis and boxplot visualization in satisfying domain specific criteria established for ensemble visualization is demonstrated. We will start the discussion with a canonical (synthetic) example and then present three more examples in prediction of hurricane tracks, medical imaging, and fluid dynamics.
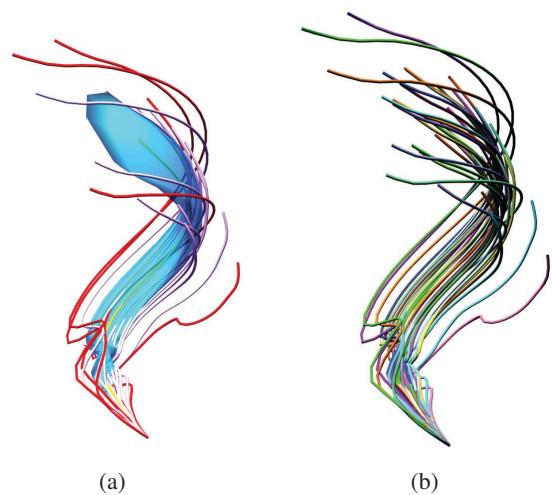

Fig. 7. Canonical ensemble data including 40 helical curves in 3D (a) Boxplot visualization. (b) Direct visualization of the ensemble members where the ensemble members are colored in random.

Our synthetic example consists of an ensemble of analytical 3D curves. The ensemble members are generated by discrete sampling of a helix equation in 3D: $h(s) = (x(s), y(s), z(s)) = (cos(s), sin(s), s)$

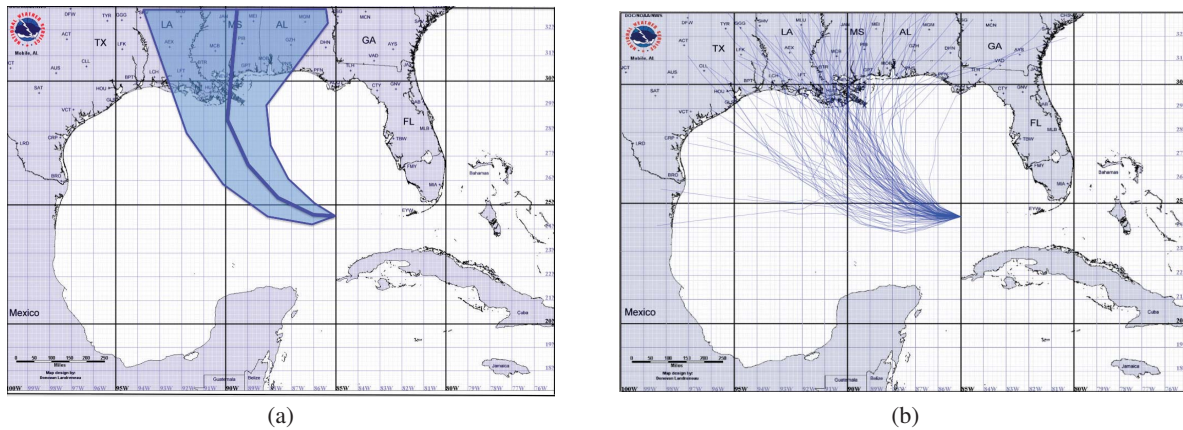| (a) | (b) |

Fig. 8. Visualization of an ensemble of 50 simulated hurricane tracks produced using the algorithm proposed by Cox *et al.* [14]: (a) The error cone: the primary public visualization provided by National Hurricane Center (NHC) [3]. (b) Direct ensemble visualization proposed by Cox *et al.* [14] in contrast to error cone visualization.

and randomly varying the position of the helical curve at the sampling positions. This example mimics the uncertainty in the position of the point along a helix generated from an uncertain 3D vector field where we considered the parameter *s* to represent time. The result of band depth analysis for our canonical example is shown in Figure 7. It can be seen that the boxplot visualization of the ensemble of 3D curves provides both qualitative and quantitative information about the variability among ensemble members while being robust in the presence of the outlying members. Note that the most representative ensemble member (*i.e.*, the sample median) is fully contained in the band.

Our first demonstrative application is analyzing and visualizing an ensemble of predicted hurricane tracks. During the life of a hurricane, the National Hurricane Center [3] issues *advisories* every six hours. These advisories usually include information about the current position of the hurricane, the wind and hurricane speed, the hurricane current bearing and a prediction about its future position and its intensity. The primary visualization provided to the public is called the *error cone* or *cone of uncertainty*, whose center represents the center of the predicted hurricane and the width is determined based on the historical forecast error of the past five years [14] (see Figure 8 (a)). The cone represents the region enclosed by two-thirds of actual hurricanes that were not predicted correctly [3], modified by the *experienced subjective* input of hurricane professionals.

Based on the observation that the error cone usually gives the wrong (public) impression about the probabilistic nature of the hurricane track predictions, an alternative visualization approach was proposed by Cox *et al.* [14]. This approach uses direct visualization of an ensemble of possible hurricane tracks generated based on the historical data and the current advisory information available. The ensemble of possible tracks is generated such that they are statistically consistent with the error cone. The visualization approach proposed by Cox *et al.* [14] is shown in Figure 8(b). Compared to the error cone visualization, the direct visualization of the possible hurricane tracks has been shown to be more informative about the uncertainty and unpredictability of the predicted hurricane track by a user study [14]. However, the user study showed that working with direct visualizations is cognitively more difficult than interpreting the error cone, thus explaining why the NHC has been hesitant to adoption (for public consumption) a spaghetti plot approach. This challenge is one of the main motivations of using alternative visualization approaches, such as the contour boxplot, instead of spaghetti plots in weather forecast applications [60].

Figure 9 demonstrates the curve boxplot visualization of the ensemble based on the data depth analysis proposed in Section 4.1 with different choices of curve parameterization. Life-time parameterization reported in Figure 9(c) is an example of application-specific parameterization. The hurricane-expert meteorologists are interested in studying the spatial variability of an ensemble of hurricane tracks over a specific period of time, for instance from the initiation until the landfall. A suitable choice of parameterization for this type of analysis

is achieved through sampling a hurricane track based on percentages of its total arc length. We denote this choice of parameterization as *life-time percentage*.

As shown in the figure, various choices of parameterization affect the sensitivity of the band depth analysis to various types of outliers. While the time-parameterization is more sensitive to the velocity outlier as a parameterization-dependent feature, the arc-length and life-time percentage parameterization are more sensitive to shape and positional outliers. The hurricane tracks whose bearing pattern is very different from the rest of the ensemble are considered as shape outliers whereas the tracks whose spatial location is far from the other members are considered as positional outlier. In addition to the aggregated statistical quantities such as outliers and the most representative hurricane track (i.e. the median), the curve boxplot also provides qualitative visualization of the spatial extent of the possible hurricane tracks by showing the 50% and 100% bands. Therefore, this visualization satisfies the criteria discussed in [14, 60].

The curve boxplot visualization in Figure 9 was presented to a group containing approximately 10 hurricane experts at the National Hurricane Center (NHC). We accomplished a "Qualitative Result Inspection" (QRI) study via a walk-through presentation of our technique with contracts to other techniques used in the literature for the same tasks [25]. We then spent a day examining the procedures used at NHC for generating their forecasts and for generating their visualizations. This one-day exercise has led to further collaboration in which members of NHC have provided us data, from which we passed back visualizations for their examination and comment. This process is ongoing. These experts were interested in the promises the curve boxplot visualization provides in enhancing analysis and visualization of ensembles in comparison to the alternative techniques currently deployed.

- These users expressed appreciation/satisfaction in the precise quantitative interpretation that is made available in these visualizations.

- The most representative ensemble member in the boxplot visualization is considered to be the member with the highest depth value. These users agreed that choosing the most representative member *from the ensemble* in comparison to other alternative aggregation techniques, such as the track generated from the mean wind fields (not necessarily a member of the ensemble), ensures that the member that is highlighted as most representative is consistent with the physical and simulation constraints. Alternatively, the *mean* track used in other visualization methods might not be a representative of the population or even physically feasible (see Figure 4 for the functional data example).

- The cognitive load of direct ensemble visualization (*e.g.* noodle or spaghetti plots) [14] currently prevents its deployment to the
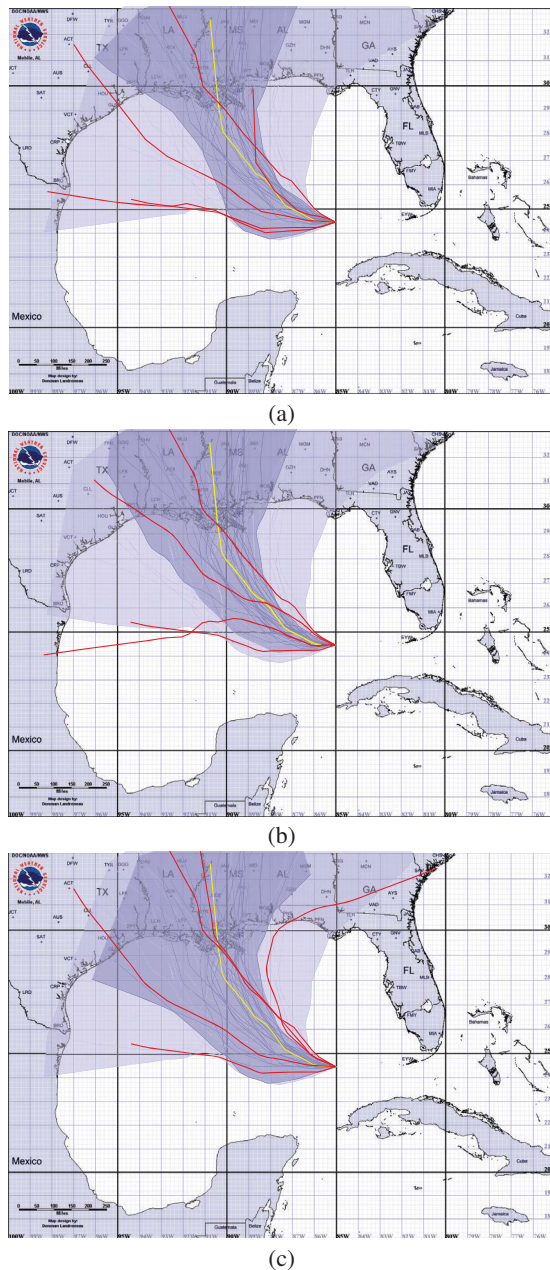
(a)

(b)

(c)

Fig. 9. Curve boxplot visualization of the ensemble of hurricane tracks presented in Figure 8 using the generalized band depth. (a) Time parameterization. (b) Arc-length parameterization. (c) Life-time percentage parameterization. The hurricane tracks are rendered in the background with the same color of the band they fall inside.
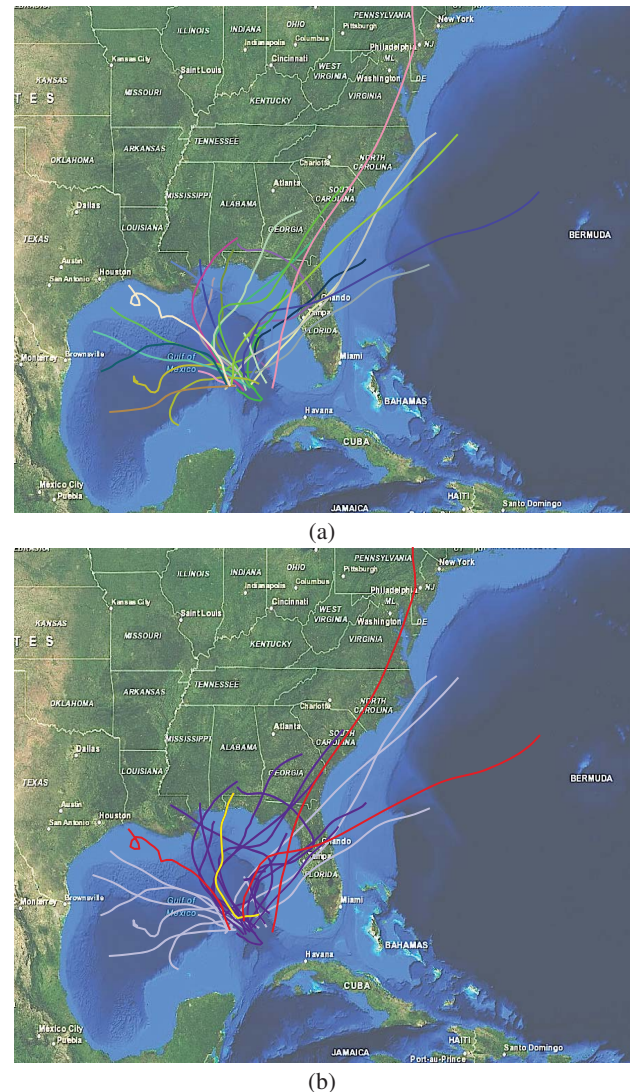

(a)

(b)

Fig. 10. 27 historic hurricane track originated in the Gulf of Mexico between 1920-2012 retrieved from historical hurricane track repository provided by NOAA [4]: (a) Direct ensemble visualization. (b) Visualization of the band depth analysis of the historic hurricane tracks using the arc-length parameterization, the tracks falling inside the 50% band are in a darker color and the tracks inside 100% band are in a lighter color.

public. On the other hand, the single aggregated quantity visualized in the cone of uncertainty may result in misinterpretation of the actual uncertainty. In comparison to these two visualization techniques, the curve boxplot provides various percentile-level information through visualization of rank statistics and bands, which these users felt may alleviate misconceptions about the meaning of the standard cone visualization.

- Outlier visualization may not be beneficial to the public. However, the visualization of outliers can be beneficial for modelers/experts who will want to understand the full variability of the model and the types of data that were excluded from the full cone.

- These users felt that the shape (and position for landfall) of the hurricane tracks was, in some instances, more important than

its speed. Thus, for certain applications they preferred the arc-length and percentage-lifetime parameterizations.

This initial qualitative domain-expert study facilitates the interest in a subsequent evaluation of the perception of curve boxplot visualization for a boarder range of audience including nonexperts and potential deployment of the curve boxplot visualization in hurricane forecast workflow.

In addition to the simulated hurricane tracks in the previous example, we also carried out the data depth analysis on an ensemble of 27 historic hurricane tracks that originated from Gulf of Mexico (a circular region of size 65 nautical miles centered at 25N by 85W) since 1920. The ensemble was retrieved from the historic hurricane track repository provided by NOAA [4]. Figure 10(a) demonstrates the direct ensemble visualization of the historic hurricane tracks as the primary visualization provided [4] and Figure 10(b) shows the visualization of the ensemble where hurricane tracks are colored based on their rank statistics induced from data depth analysis. Coloring individual tracks based on their depth values is considered as a simple alternative visualization to boxplot visualization. The arc-length parameterization used for the hurricane tracks is adopted from the previ-

ous example where the life cycle of the hurricanes for this example is 96 hours. Note that median as the most representative ensemble members has a landfall near Pensacola in Florida and the hurricane tracks falling inside the 50% band mainly head toward west Florida which is consistent with hurricane-risk analysis for the Gulf Coast [2].
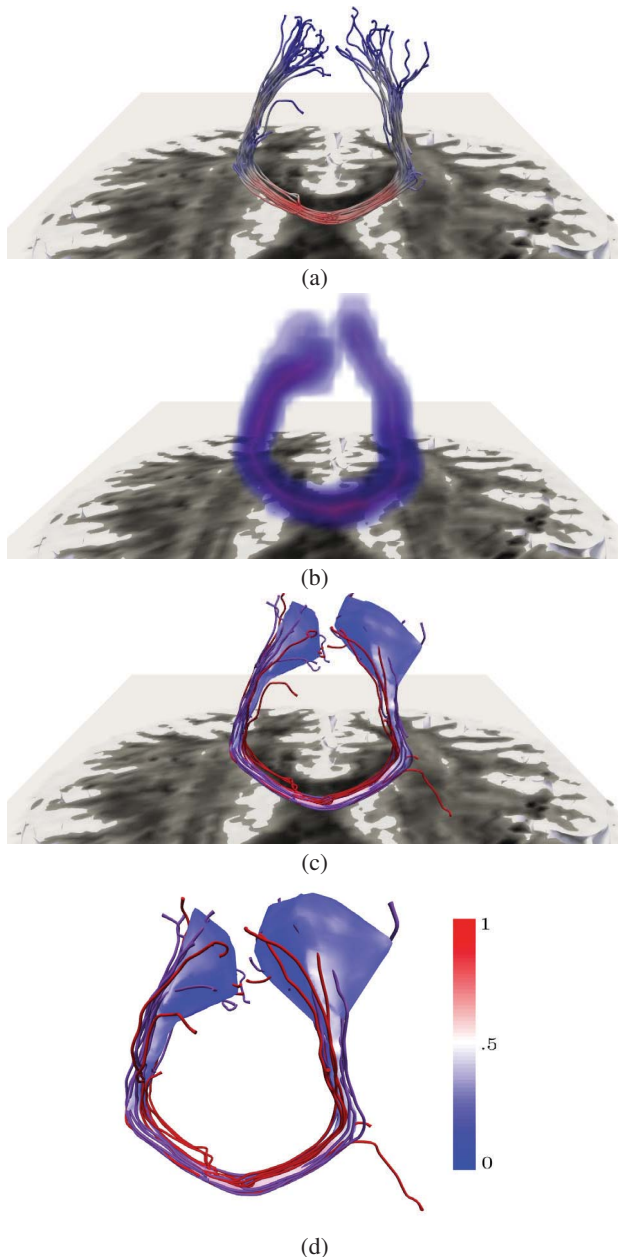

Fig. 11. Ensemble of tracts originated from 50 seed points at the center of the corpus callosum using the Camino toolkit [13]. (a) Direct visualization of the ensemble where the tracts are colored based on FA values using the colormap presented. Lower FA values correspond to more isotropic diffusion while higher values correspond to more anisotropic or directional diffusion (b) Probability connection map of the ensemble of tracts. (c) Boxplot visualization of the tracts: the 50% band is colored based on FA values using the colormap presented. (d) Zoomed in view of the boxplot visualization along with the colormap used.

Our third set of experimental results is motivated by applications of the proposed method in medical imaging. The connectivity between different locations inside the brain is studied in medical applications in order to reconstruct the neurological function of different regions of the brain. Tractography algorithms are among the most widely used

methods to infer these connectivities. Tractography algorithms generate particle trace pathlines in terms of parameterized curves (also known as *tracts*) by propagating trajectories from specified seed points inside the brain based on direction information extracted from diffusion weighted magnetic resonance imaging (DW-MR). The directional information is based on the anisotropy of the diffusion process at each voxel of the image. A scalar map called the fractional anisotropy (FA) map is often used to specify the degree of anisotropy of a diffusion process at each location of the image. A value close to 0 on the FA map corresponds to free or equally-likely diffusion in all directions and value 1 specifies a directional diffusion.

The directional information from the DW-MR imaging is prone to errors. As a result, there have been different efforts in using probabilistic approaches to follow multiple trajectories initiated in a specific part of the brain [18, 27, 49] to account for different sources of error including noise and orientation dispersion. The probabilistic tractography will result in a collection of streamlines or tracts from each seed location in the brain that account for the underlying uncertainty in the exact location of the neural fiber tracts in the brain. We have used the Camino diffusion MRI Toolkit [13] to generate an ensemble of probabilistic tracts at the center of the corpus callosum. In Figure 11, we have shown the boxplot visualization of the ensemble of tracts along with two other benchmark methods widely used to study tractography data. For this example, we used the curve-parameterization provided by Camino [13].

The first method is direct visualization of the tracts in which each point on the tract has been colored based on the corresponding value on the FA map (Figure 11(a)). The second method, shown in Figure 11(b), is called the connection probability map. The connection probability map depicts the probability of the existence of a connection between a specific voxel to another voxel of the image, and it is widely used in the medical imaging community for this purpose [41, 7]. The probability connection map provides little information about how or where the tracts undergo an increase in variability (diverge). On the other hand, the direct visualization provides more insight about how the tracts diverge as they leave the seed points, but does not provide any quantitative information about the variability. Finally, the boxplot visualization of the 50% band in Figure 11(c-d) clearly shows that the tracts start as a bundle and their dispersion significantly increases as the FA values drop. This has been verified by shading the surface of the band based on the values of the FA map. We see that the 50% band remains narrow in the regions with high values of FA (shaded in red). The 50% band widens as the corresponding FA values decrease, and expands significantly where the FA values are low (shaded in blue). The most representative member is fully contained in the band and therefore, is not visible in this particular visualization. Illustrative confidence intervals based on distance-based confidence measures has been previously proposed to study the variation present in an ensemble [10]. Data depth analysis can provide robust confidence values in comparison with distance-based measures specially in presence of different types of outliers. Moreover, the boxplot visualization proposed not only provides information regarding the confidence intervals but also present most representative and outlying members.

Our last example is a fluid simulation application. Pathlines and streamlines are widely used in fluid dynamics to study the presence and evolution of structures such as vortices [6]. Among various parameters involved in the formation of vortices in the fluid flow, the effect of Reynolds number and the boundary conditions such as inlet velocity are of interest. We used the 2D incompressible Navier-Stokes solver as part of the Nektar++ software package [1] to generate an ensemble of size 30, where the Reynolds number and the inlet velocity have been chosen randomly for various simulation runs. For this demonstration, the velocity field in 2D along with analytically calculated vorticity values (*i.e.*, orthogonal to the velocity field by definition) were used to generate the full 3D vector field. An ensemble of pathlines was then generated by placing a seed point close to the surface of the cylinder. The direct ensemble visualization and the boxplot visualization based on time parameterization are depicted in Figure 12. In this visualization we see the oscillatory nature of pathlines along the eddy line due
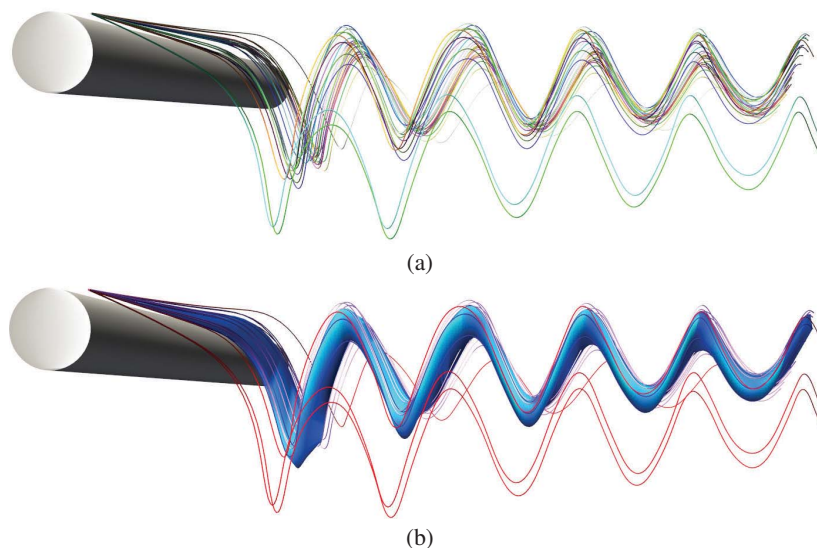
(a)

(b)

Fig. 12. An ensemble of 30 particle trace pathlines derived from the 3D vector field of a fluid flow around a cylinder. For demonstration purposes, the vorticity (along z) is constructed and populated from the 2D velocity field analytically. (a) Direct visualization of the ensemble. (b) Boxplot visualization of the ensemble.

to the vortex behavior. We also see that the ensemble presents a coherent set of frequencies of oscillation, with the exception of a few outliers that have different positions and shapes. We also see a great deal of variation in the depths of these pathlines, demonstrating a relatively greater variation in vorticity as we move down the eddy line.

For all the results in this paper, the band depth analysis has been implemented in C++. The band inclusion tests were implemented using open source geometry libraries (VTK and CGAL). The data depth computations were performed on a quad core (3.20 GHz) desktop computer. The data depth computations are independent and have been parallelized using the OpenMP API. However, no optimization has been carried out for the computation and evaluation of band inclusion checks associated with Eq. (8). Therefore, the performance of the algorithm can be significantly improved up to interactive speed through proper parallelization of this stage and more efficient computations [12]. The computation time also depends on the dimensionality of the data. With the current implementation, an ensemble consisting of 50 2D hurricane tracks with average length of 60 sample points along each pathline would take approximately 1 minute, whereas for 3D cases, the computational time is dominated by the computations involved in Eq. (8) and might take up to 20 minutes on a desktop computer with specifications given above.

6 CONCLUSION & FUTURE WORK

Robust statistical analysis and visualization of an ensemble of multivariate curves, having minimal assumptions about the underlying distribution, is a challenging task – specifically in situations where both spatial and global geometrical features are of interest. In this paper, we presented a nonparametric method of deriving robust and descriptive statistical information from an ensemble of multivariate curves based on the notion of data depth. A generalization of the boxplot visualization strategy in 2D and 3D has been also proposed to visualize the main features based on the order statistics inferred from the ensemble. Unlike many other strategies, our work is robust to outliers. We have demonstrated the utility of both a data depth analysis and a boxplot visualization for ensembles of multivariate curves in various applications. We have provided a comparison against other state-of-the-art approaches. We discussed how one can attain the desirable, established criteria within each application, as opposed to the other methodologies, to accomplish the challenging task of ensemble visualization. We have also provided qualitative feedback from domain experts in our hurricane prediction application.

Some of the limitations of the proposed method shed light on potential research directions for future work. For example, the present method is not able to provide representative features of an ensemble generated by a multimodal distribution; therefore, studying and visualizing descriptive statistics for ensembles generated from a multimodal distributions still require further investigation. For instance, complex branching structures can emerge in curve ensembles generated from a multimodal distribution. Defining a parameterization-invariant notion of band depth is still an open and challenging problem. The main assumption in band depth analysis for various types of data is the establishment of the correspondence over the domain. Geometrically, the band formed by multivariate curves can be thought of as a polytope in higher dimensions. Therefore, simplicial tessellation of this region can be used to define the band. However, efficient construction of this region remains a challenge.

REFERENCES

[1] Nektar++, 2012. http://www.nektar.info.
[2] Hurricane Hotspots, 2014. http://www.bestplaces.net/docs/studies/hurricane_hotspots.aspx, Last visited March 17, 2014.
[3] National Hurricane Center, 2014. http://www.nhc.noaa.gov.
[4] National Oceanic and Atmospheric Administration Historical Hurricane Tracks, 2014. http://csc.noaa.gov/hurricanes, Last visited March 13, 2014.
[5] H. Alt, C. Knauer, and C. Wenk. Comparison of distance measures for planar curves. *Algorithmica*, 38(1):45–58, 2004.
[6] G. K. Batchelor. *An Introduction to Fluid Dynamics*. Cambridge University Press, 2000.
[7] T. E. Behrens, M. W. Woolrich, M. Jenkinson, H. Johansen-Berg, R. G. Nunes, S. Clare, P. M. Matthews, J. M. Brady, and S. M. Smith. Characterization and propagation of uncertainty in diffusion-weighted mr imaging. *Magn Reson Med*, 50(5):1077–88, 2003.
[8] P. Bickel and E. Lehmann. Descriptive statistics for nonparametric models i. introduction. In *Selected Works of E. L. Lehmann*, Selected Works in Probability and Statistics, pages 465–471. Springer US, 2012.
[9] R. P. Botchen, D. Weiskopf, and T. Ertl. Interactive visualisation of uncertainty in flow fields using texture-based techniques. In *12th International Symposium on Flow Visualisation*, 2006.

[10] R. Brecheisen, B. Platel, B. M. Haar Romeny, and A. Vilanova. Illustrative uncertainty visualization of dti fiber pathways. *The Visual Computer*, 29(4):297–309, 2013.

[11] E. W. Chambers and Y. Wang. Measuring similarity between curves on 2-manifolds via homotopy area. *Symposium on Computational Geometry*, pages 425–434, 2013.

[12] A. Y. Cheng and M. Ouyang. On algorithms for simplicial depth. In *Canadian Conference on Computational Geometry*, pages 53–56, 2001.

[13] P. A. Cook, Y. Bai, N. S. Gilani, K. K. Seunarine, M. G. Hall, G. J. Parker, and D. C. Alexander. Camino: Open-source diffusion-MRI reconstruction and processing. *14th Scientific Meeting of the International Society for Magnetic Resonance in Medicine*, pages 2759+, May 2006.

[14] J. Cox, D. House, and M. Lindell. Visualizing uncertainty in predicted hurricane tracks. *International Journal for Uncertainty Quantification*, 3(2):143–156, 2013.

[15] S. Djurcilov, K. Kim, P. Lermusianax, and A. Pang. Visualizing scalar volumetric data with uncertainty. *Comp. and Graph.*, 26:239–248, 2002.

[16] D. L. Donoho and M. Gasko. Breakdown properties of location estimates based on halfspace depth and projected outlyingness. *The Annals of Statistics*, 20(4):1803–1827, 12 1992.

[17] A. Efrat, Q. Fan, and S. Venkatasubramanian. Curve matching, time warping, and light fields: New algorithms for computing similarity between curves. *Journal of Math. Img. and Vis.*, 27(3):203–216, 2007.

[18] O. Friman, G. Farneback, and C.-F. Westin. A Bayesian approach for stochastic white matter tractography. *IEEE Trans. Med. Img.*, 25(8):965–978, 2006.

[19] O. Friman, A. Hennemuth, A. Harloff, J. Bock, M. Markl, and H.-O. Peitgen. Probabilistic 4D blood flow tracking and uncertainty estimation. *Medical Image Analysis*, 15(5):720–728, 2011.

[20] S. Gaffney and P. Smyth. Joint probabilistic curve clustering and alignment. In *Advances in Neural Information Processing Systems*, 2004.

[21] M. G. Genton, C. Johnson, K. Potter, and a. S. Georgiy Stenchikov. Surface boxplots. *The ISI Journal for the Rapid Dissemination of Statistics Research*, 2013.

[22] G. Grigoryan and P. Rheingans. Probabilistic surfaces: Point based primitives to show surface uncertainty. In *Proceedings of IEEE Visualization*, pages 147–153, 2002.

[23] G. Grigoryan and P. Rheingans. Point-based probabilistic surfaces to show surface uncertainty. *IEEE Trans. Vis. Comput. Graph.*, 10:564–573, 2004.

[24] M. Hummel, H. Obermaier, C. Garth, and K. I. Joy. Comparative visual analysis of lagrangian transport in cfd ensembles. *IEEE Trans. Vis. Comput. Graph.*, 19(12):2743–2752, 2013.

[25] T. Isenberg, P. Isenberg, J. Chen, M. Sedlmair, and T. Móller. A systematic review on the practice of evaluating visualization. *EEE Trans. Vis. Comput. Graph.*, 19(12):2818–2827, 2013.

[26] C. Johnson and A. Sanderson. A next step: Visualizing errors and uncertainty. *IEEE Comp. Graph. and App.*, 23:6–10, 2003.

[27] D. K. Jones. Tractography gone wild: Probabilistic fibre tracking using the wild bootstrap with diffusion tensor mri. *IEEE Trans. Med. Imaging*, 27(9):1268–1274, 2008.

[28] D. G. Kendall. A survey of the statistical theory of shape. *Statistical Science*, 4(2):87–99, 1989.

[29] A. Kuhn, N. Lindow, T. Günther, A. Wiebel, H. Theisel, and H.-C. Hege. Trajectory density projection for vector field visualization. *EuroVis - Short Papers*, pages 31–35, 2013.

[30] R. Liu. On a notion of data depth based on random simplices. *The Annals of Statistics*, 18:405–414, 1990.

[31] S. Lodha, C. Wilson, and R. Sheehan. Listen: sounding uncertainty visualization. In *Proceedings of IEEE Visualization*, pages 189–195, November 1996.

[32] S. K. Lodha, A. Pang, R. E. Sheehan, and C. M. Wittenbrink. Uflow: Visualizing uncertainty in fluid flow. In *IEEE Visualization*, pages 249–254, 1996.

[33] S. López-Pintado and J. Romo. On the Concept of Depth for Functional Data. *Journal of the American Statistical Association*, 104(486):718–734, 2009.

[34] S. López-Pintado, Y. Sun, J. Lin, and M. Genton. Simplicial band depth for multivariate functional data. *Advances in Data Analysis and Classification*, pages 1–18, 2014.

[35] I. Lyu, S. Kim, J.-K. Seong, S. Yoo, A. Evans, Y. Shi, M. Sanchez, M. Niethammer, and M. Styner. Group-wise cortical correspondence via sulcal curve-constrained entropy minimization. In *Information Processing in Medical Imaging*, volume 7917, pages 364–375, 2013.

[36] S. Marchesin, C.-K. Chen, C. Ho, and K.-L. Ma. View-dependent streamlines for 3D vector fields. *IEEE Trans. Vis. Comput. Graph.*, 16(6):1578–1586, 2010.

[37] T. McLoughlin, M. W. Jones, R. S. Laramee, R. Malki, I. Masters, and C. D. Hansen. Similarity measures for enhancing interactive streamline seeding. *IEEE Trans. Vis. Comput. Graph.*, 19(8):1342–1353, 2013.

[38] M. Otto, T. Germer, and H. Theisel. Closed stream lines in uncertain vector fields. In *Proceedings of the 27th Spring Conference on Computer Graphics*, SCCG '11, pages 87–94. ACM, 2013.

[39] M. Otto and H. Theisel. Vortex analysis in uncertain vector fields. *Comput. Graph. Forum*, 31(3):1035–1044, 2012.

[40] A. Pang, C. Wittenbrink, and S. Lodha. Approaches to uncertainty visualization. *The Visual Computer*, 13:370–390, 1997.

[41] G. J. Parker and D. C. Alexander. Probabilistic monte carlo based mapping of cerebral connections utilising whole-brain crossing fibre information. *Information processing in medical imaging*, 18:684–695, 2003.

[42] C. Petz, K. Pöthkow, and H.-C. Hege. Probabilistic local features in uncertain vector fields with spatial correlation. *Comput. Graph. Forum*, 31:1045–1054, 2012.

[43] T. Pfaffelmoser, M. Reitinger, and R. Westermann. Visualizing the positional and geometrical variability of isosurfaces in uncertain scalar fields. *Comput. Graph. Forum*, 30(3):951–960, 2011.

[44] T. Pfaffelmoser and R. Westermann. Visualization of global correlation structures in uncertain 2D scalar fields. In *Comput. Graph. Forum*, volume 31, pages 1025–1034. Wiley Online Library, 2012.

[45] K. Pöthkow and H.-C. Hege. Nonparametric models for uncertainty visualization. *Comput. Graph. Forum*, 32(3):131 – 140, 2013.

[46] K. Pöthkow, C. Petz, and H.-C. Hege. Approximate level-crossing probabilities for interactive visualization of uncertain isocontours. *International Journal for Uncertainty Quantification*, 3(2):101–117, 2013.

[47] K. Pöthkow, B. Weber, and H.-C. Hege. Probabilistic marching cubes. *Comput. Graph. Forum*, 30(3):931–940, 2011.

[48] P. J. Rousseeuw, I. Ruts, and J. W. Tukey. The bagplot: A bivariate boxplot. *The American Statistician*, 53(4):382–287, November 1999.

[49] M. Rowe, H. G. Zhang, N. Oxtoby, and D. C. Alexander. Beyond crossing fibers: tractography exploiting sub-voxel fibre dispersion and neighbourhood structure. In *Proceedings of the 23rd international conference on Information Processing in Medical Imaging*, pages 402–413, 2013.

[50] C. J. Roy and W. L. Oberkampf. A comprehensive framework for verification, validation, and uncertainty quantification in scientific computing. *Computer Methods in Applied Mechanics and Engineering*, 200(2528):2131 – 2144, 2011.

[51] J. Sanyal, S. Zhang, J. Dyer, A. Mercer, P. Amburn, and R. Moorhead. Noodles: A tool for visualization of numerical weather model ensemble uncertainty. *IEEE Trans. Vis. Comput. Graph.*, 16(6):1421–1430, 2010.

[52] T. B. Sebastian, P. N. Klein, and B. B. Kimia. On aligning curves. *IEEE Trans. Pattern Anal. Mach. Intell.*, 25(1):116–124, 2003.

[53] A. Srivastava, E. Klassen, S. H. Joshi, and I. H. Jermyn. Shape analysis of elastic curves in euclidean spaces. *IEEE Trans. on Pattern Analysis and Machine Intelligence*, 33(7):1415–1428, 2011.

[54] Y. Sun and M. G. Genton. Functional boxplots. *Journal of Computational and Graphical Statistics*, 20(2):316–334, June 2011.

[55] J. W. Tukey. Mathematics and the picturing of data. In *International Congress of Mathematicians 1974*, volume 2, pages 523–532, 1974.

[56] J. W. Tukey. *Exploratory Data Analysis*. Addison-Wesley, 1977.

[57] V. Verma and A. Pang. Comparative flow visualization. *IEEE Trans. Vis. Comput. Graph.*, 10(6):609–624, 2004.

[58] H. Wang, J. Kearney, and K. Atkinson. Arc-length parameterized spline curves for real-time simulation. In *Proc. 5th International Conference on Curves and Surfaces*, pages 387–396, 2002.

[59] D. Weiskopf and G. Erlebacher. Overview of flow visualization. In C. D. Hansen and C. R. Johnson, editors, *The Visualization Handbook*, pages 261–278. Elsevier, Amsterdam, 2005.

[60] R. T. Whitaker, M. Mirzargar, and R. M. Kirby. Contour boxplots: A method for characterizing uncertainty in feature sets from simulation ensembles. *IEEE Trans. Vis. Comput. Graph.*, 19(12):2713–2722, 2013.

[61] H. Yu, C. Wang, C.-K. Shene, and J. H. Chen. Hierarchical streamline bundles. *IEEE Trans. Vis. Comput. Graph.*, 18(8):1353–1367, 2012.

[62] Y. Zuo and R. Serfling. General notions of statistical depth function. *Ann. Statist*, 28:461–482, 2000.